Title:

Experimental evolution toward extinction in a molecular host-parasite system

Authors:

Kohtoh Yukawa[1], Tomoaki Yoshiyama[2], Ryo Mizuuchi[3], Norikazu Ichihashi[*1,4,5]

Affiliations:

[1]Department of Life Science, Graduate School of Arts and Science, The University of Tokyo, Meguro, Tokyo 153-8902, Japan

[2]Graduate School of Information Science and Technology, Osaka University.

[3]Department of Electrical Engineering and Bioscience, Faculty of Science and Engineering, Waseda University, Shinjuku, Tokyo 162-8480, Japan.

[4]Komaba Institute for Sciences, The University of Tokyo, Meguro, Tokyo 153-8902, Japan

[5]Universal Biology Institute, The University of Tokyo, Meguro, Tokyo 153-8902, Japan

Correspondence:

Norikazu Ichihashi

Department of Life Science, Graduate School of Arts and Science, The University of Tokyo, 3-8-1 Komaba, Meguro-ku, Tokyo 153-8902, Japan

Tel: 81-3-5465-7307; Fax: 81-3-5465-7307; Email: ichihashi@g.ecc.u-tokyo.ac.jp

Keywords:

Self-replicator, parasite, oscillation, coevolution, diversity, extinction

Abstract

Theoretical studies have proposed that coevolution with parasitic replicators plays a critical role in the evolution of primitive life; however, experimental verification of the potential outcomes of such coevolutionary dynamics remains limited. We previously conducted a co-evolutionary experiment using an RNA-protein replication system that resulted in the spontaneous diversification of host and parasitic RNA into five distinct lineages with robust co-replication. Here, we report contrasting evolutionary outcomes from a second long-term co-evolutionary experiment. Using a flow reactor system with increased dilution frequency over 5000 h (15,000 generations), we observed reduced diversity and frequent extinctions in later experimental stages. Co-replication assays of RNA clones revealed that the primary cause of this diversity loss was shortened reaction time due to frequent dilution. Further analysis of RNA clones that emerged during evolution suggested that the frequent extinctions resulted from the dominance of host species that had either lost parasite resistance or exhibited reduced replication ability. These findings demonstrate that co-evolution between host and parasitic replicators can result in diversity loss and frequent extinctions depending on dilution conditions, highlighting the critical role of environmental parameters, such as dilution frequency, in enabling primitive replicators to evolve sustainably toward the emergence of life.

Main

Introduction

Many scenarios for the origins of life propose that self-replicating molecules, such as self-replicating RNA, acquired the ability of Darwinian evolution in the ancient Earth and subsequently evolved through increasing complexity and diversity to approach extant life[1–9]. However, whether and how self-replicating molecules can spontaneously develop diversity and complexity through evolutionary processes remains largely unknown.

One promising approach involves experimental evolution using replicating molecules capable of evolution. The first experimental molecular evolution was reported in 1967 by Spiegelman's group, in which phage genomic RNA was replicated by purified phage RNA replication enzyme (replicase) across multiple generations[10]. Subsequently, other RNA/DNA replication systems were developed and employed for experimental evolution[11,12]. Although these systems demonstrated biologically relevant

phenomena, including niche differentiation[13] and adaptation to inhibitory chemicals[14,15], the typical evolutionary outcome was dominance by the fastest replicators under given conditions, with no observed diversification.

Contrasting results were obtained when a translation system was integrated with Spiegelman's RNA replication system (designated the translation-coupled RNA replication system) in our previous study[16]. In this system, RNA encoding an RNA replicase is replicated by the RNA replicase translated from itself in a reconstituted E. coli translation system (Fig. 1a). A notable feature of this system is the emergence of parasitic RNAs that have lost the replicase-encoding sequence while retaining the replicase recognition sequence through RNA recombination. These parasitic RNAs replicate by exploiting "host" RNAs that retain the replicase gene but replicate significantly faster than host RNAs due to their reduced size. To prevent excessive amplification of parasitic RNAs, the system was compartmentalized within water-in-oil droplets. Through serial dilution cycles, the RNA sustained replication and continued evolving. In previous long-term evolutionary experiments more than 500 generations, we observed co-evolution of host and parasitic RNAs through an evolutionary arms race[17], wherein the ancestral host RNA diversified into at least five distinct lineages—three host lineages and two parasite lineages—forming an interdependent replication network[18].

One factor contributing to the distinct evolutionary outcomes in the translation-coupled RNA replication system may be the emergence of parasitic entities. Parasitic molecules have been considered a critical obstacle for primitive self-replicators to overcome prior to the emergence of life, as parasites inevitably arise in self-replicating systems[19] and disrupt interdependent or cooperative replication networks[20,21]. Several solutions to this problem have been proposed, including compartmentalization, whether permanent or transient[22–28], limited dispersion[29–35], molecular kin selection[36], and physical linkage evolution[37]. Even when the problem of parasite amplification is resolved through these mechanisms, how hosts and parasites co-evolve remains an open question.

Theoretical studies have predicted diverse coevolutionary outcomes (reviewed in [38]) and some are related to primitive replicators: increased host diversity and complexity[39–42], enhanced host variation with stabilized oscillation dynamics[43], or extinctions of a host species due to reduced population sizes during oscillations[44]. While many coevolutionary experiments using extant organisms have been conducted (reviewed in [45]), these studies employed relatively short time scales compared to the theoretical frameworks for primitive replicators mentioned above, and theoretical predictions regarding diversification and extinction dynamics remain insufficiently verified. In our

aforementioned long-term coevolutionary experiment using the translation-coupled RNA replication system, we observed stable coexistence and divergence of host and parasitic RNAs[18,46]. However, whether this evolutionary outcome consistently occurs in this system or whether alternative outcomes are possible under different conditions remains unknown.

In this study, we conducted another long-term evolutionary experiment up to 15,000 generations under increased serial dilution frequency using a flow reactor system and observed a contrasting coevolutionary outcome: evolution toward reduced diversity and periodic extinction. During the early phase of evolution, host and parasitic RNA continued replicating with oscillatory dynamics similar to our previous experiment; however, in later phases, host RNA concentrations frequently declined substantially and became undetectable (i.e., underwent extinction). We also observed that the diversified host and parasite lineages present in the initial population were eliminated shortly after starting this evolutionary experiment, with only one host and one parasite lineage persisting in later stages. Short-term replication assays using cloned host and parasitic RNAs indicated that diversity loss resulted from shortened reaction times caused by frequent dilution, while periodic extinctions were attributed to reduced parasite resistance or reduced host replication ability.

Result

Evolutionary experiment with a flow-reactor system

For another evolutionary experiment utilizing an automated format, we employed a previously developed droplet flow reactor system[47]. In this system, droplets containing the translation system were supplied to the reactor at a constant rate. Within the reactor, droplets, which contains host and parasitic RNAs, were stirred at a specified frequency to induce fusion and division events, thereby mixing the contents and enabling RNA to continue replication. Details of the flow reactor system are presented in Fig. S1. The difference between the new flow reactor (FR) condition and the previous manual serial dilution (SD) condition is illustrated in Fig. 1b. Under SD condition, each serial dilution cycle consisted of 5-h incubation at 37°C, followed by 5-fold dilution with fresh oil and the translation system. The diluted droplets were vigorously mixed using a homogenizer to achieve nearly complete mixing of the contents of droplets, then incubated for the subsequent replication cycle. Under FR condition, the reaction mixture was continuously diluted to exchange 20% of the tank volume per hour, while a magnetic stirrer periodically induced droplet mixing at approximately two fusion-division

events per hour.

Using this FR system, we conducted a long-term evolutionary experiment employing the RNA population from round 155 of our previous evolutionary experiment under SD condition, in which RNA had already diversified into three host and one parasite lineage. Host RNA concentrations were quantified by reverse transcription followed by quantitative PCR (RT-qPCR). Figure 1c presents host RNA concentrations for both the previous evolutionary experiment under SD condition (light green lines) and the current experiment under FR condition (dark green lines). Under both conditions, host RNA concentrations exhibited oscillatory dynamics; however, the average RNA concentration under FR condition was lower than under SD condition. Host RNA continued to be detected for approximately 2000 h under FR condition, but undetected (i.e., extinct) after 2264 h (top panel in Fig. 1c). We restarted the experiment using preserved droplets from 1920 h (indicated by the red dotted line). Then, host RNA replication persisted slightly longer, suggesting that extinction was stochastic, but again became undetectable after 2600 h (second panel from top). In this way, we continued evolutionary experiment until 5024 h and experienced extinctions eight times in total. Extinctions occurred frequently in later experimental phases, particularly around 2000, 3000, and 4500 h, suggesting that RNA populations evolved during these periods may possess characteristics that induce them to extinction.

The complete trajectory of RNA concentration for the experiment with the longest duration up to 5000 h (corresponding to 15,000 generations, see Method for calculation) is presented in the bottom panel of Fig. 1c. For this experiment, we also quantified parasitic RNA concentrations (purple marks) based on band intensity following polyacrylamide-gel electrophoresis (Fig. S2). The detection limit for the band intensity method is substantially higher than that of RT-qPCR employed for host RNA quantification; consequently, parasitic RNA was detectable only at elevated concentrations. Parasites were detected intermittently around host RNA concentration peaks, indicating that parasite RNA concentrations also oscillated in accordance with host oscillations. In subsequent analyses, we examined RNA populations from this longest-duration evolutionary experiment.

Sequence analysis

To elucidate the evolutionary dynamics of hosts and parasites during the FR evolutionary experiment, we analyzed host and parasite RNA sequences at nine time points (red stars in Fig. 1c) using long-read

deep sequencing (PacBio Sequel) after reverse-transcription. To eliminate the effect of sequence error and quasispecies, we identified dominant mutations occurring at frequencies of 10% or higher at least one analyzed time point and classified sequences into genotypes based on the presence or absence of these dominant mutations (Figs. S3 and S4). We constructed a phylogenetic tree incorporating the three most abundant genotypes at each analyzed time point (solid lines in Fig. 2a), along with the data before round 155 of the previous SD evolutionary experiment (dotted lines). We also presented the frequency of each genotype as a heatmap aligned with the phylogenetic tree.

At the starting point (0 h) of the FR experiment (i.e., round 155 of the SD experiment), three host lineages (HL1, HL2, and HL3) and one parasite lineage (PL2) were present (Fig. 2). However, after 480 h, HL2 and HL3 disappeared, with only one host (HL1) and one parasite (PL2) remaining detectable, indicating that diversified lineages were not sustained under FR condition. The existence of each lineage is schematically shown at the top of the heatmap. The heatmap additionally reveals a relatively homogeneous population consisting of closely related branches until 5000 h, differing by only 2-3 mutations in the host population shown in Fig. 2. This result indicated that new distinct lineages did not emerge under FR condition. These results under FR condition represent a stark contrast to the previous SD experiment (Fig. S5), in which five distinct lineages emerged.

Conditions for maintaining diversity

We investigated the differences between FR and SD conditions that influence diversity maintenance (i.e., the number of coexisting RNA species). The two primary differences between FR and SD conditions were 1) the continuous reaction time that RNA experienced prior to dilution and 2) the dilution rate following the reaction. We hypothesized that these differences affect the number of coexisting RNA species. To test this hypothesis, we conducted short-term replication experiments employing serial dilution method using multiple RNA species at varying reaction times and dilution rates, including those corresponding to FR and SD conditions, then evaluating the number of RNA species present in the final population.

The reaction time and dilution rate under SD condition are corresponding to 5 h and 0.8/round, respectively because RNA experienced continuous incubation for 5 h before dilution and then diluted 5-fold (Fig. 1b, left). Under FR condition, RNA in the droplets should have experienced continuous

incubation for 0.5 h before dilution on average because droplets underwent two fusion-division events per hour (Fig. 1b, right). Assuming same sizes for all droplets, the dilution rate at the fusion-division event should be 0.5. Therefore, we decided the reaction time and dilution rate under FR condition are close to 0.5 h and 0.5/round, respectively (more detailed rationale for this calculation is described in Method section).

As RNA species for this experiment, we initially selected four RNA species from round 155 (HL1, 2, 3, and PL2); however, these did not exhibit stable co-replication (Fig. S6), likely because these RNAs had not yet established stable interdependencies. We therefore employed five RNA clones from a later round—three host RNAs (HL1, HL2, and HL3) and two parasitic RNAs (PL2 and PL3)—identified at round 228 in the previous study[18], in which four of these five RNA species (excluding HL3) demonstrated co-replication under SD condition (5 h reaction time and 0.8 /round dilution rate).

Prior to conducting the experiments, we investigated the effect of reaction time and dilution rate on the number of co-replicable RNA species using mathematical modeling and simulation. This mathematical model was based on a previous study[46]. The model comprised three sequential steps: 1) RNA replication reactions dependent on the number of RNA molecules within each droplet, 2) random removal and supply of droplets (dilution), and 3) random fusion-division of droplets (see Methods for details). In these simulations, we varied the reaction time for RNA replication (0.5, 1, and 5 h) and the dilution rate (0.5, 0.8, 0.9, and 0.99 per round). Other parameters, including the replication rate of each RNA species, were derived from experimentally determined values[18]. We executed 50 rounds of the replication-dilution-fusion-division cycle 20 times. Representative RNA concentration dynamics are presented in Fig. 3a. The average number of remaining RNA species in final populations is displayed in the upper left triangle of Fig. 3c.

To validate these results, we conducted nine short-term serial dilution experiments at varying reaction times and dilution rates and quantified the concentration of each RNA species using specific RT-qPCR (Fig. 3b). The number of maintained RNA species in the final 40-50 rounds is presented in the bottom right panel of Fig. 3c. The number of remaining RNA species was significantly dependent on both reaction time and dilution rate, with simulation and experimental results exhibiting similar trends. At

205 shorter reaction times and higher dilution rates (upper-left region of Fig. 3c), RNA species rarely
206 persisted, whereas at longer reaction times and lower dilution rates and (lower-right region), greater
207 numbers of RNA species were maintained. Specifically, under the previous SD evolutionary condition
208 (5 h reaction and 0.8/round dilution, green dotted square), 3.6 - 4 RNA types were sustained. Under
209 the condition corresponding to the FR evolutionary experiment (5 h reaction and 0.5/round dilution,
210 blue dotted square), only 1.6-3 RNA species persisted, consistent with the loss of pre-existing RNA
211 diversity during the FR evolutionary experiment shown in Fig. 2, where two RNA lineages remained.
212 These results suggest that reduced diversity under FR condition can be primarily attributed to shorter
213 reaction times because another difference under FR condition, reduced dilution rate, should increase
214 the diversity at the reaction time of 0.5 h based on the data of Fig. 3c. Additional discussion is provided
215 in Supplemental Discussion.

216

217 **Cause of extinction**

218 We investigated the underlying cause of host RNA disappearance during later stages of the
219 evolutionary experiment. Such disappearance may be directly attributed to reduced host RNA
220 concentrations at the bottom of the oscillation dynamics, which likely results in stochastic removal of
221 all host RNA molecules from the reactor. If this hypothesis is correct, host RNA concentrations at the
222 bottom should decrease in the later stage of evolution. To test this, we plotted RNA concentrations at
223 each bottom of the oscillation in Fig. 4a (blue points), which were approximately 10^{-3} nM during 0-
224 1000 h and decreased to 10^{-4} nM during 1000-2000 h and 3000-4600 h. Beyond 4600 h, the bottom
225 concentrations decreased further.

226

227 Next, we investigated whether evolved host and parasite RNAs in later stages exhibited characteristics
228 that reduced host concentrations at the bottom of oscillation. We selected the most frequent host
229 sequences at nine time points (0, 480, 1152, 1520, 2064, 2848, 3376, 3984, and 4616 h) and prepared
230 individual RNA clones. For parasite, we selected five major sequences that were identical during 1152-
231 2064 h and 2848-3376 h because similar sequences were sustained for relatively long periods. At 4616
232 h, parasitic RNA was undetectable; therefore, we employed the sequence from 3984 h. Using these
233 host-parasite pairs from each time point (1 nM each), we conducted single-round competition
234 experiments and quantified RNA replication (Fig. 4b).

For the initial host-parasite pair prior to the FR evolutionary experiment, the host replicated selectively without parasite amplification (Fig. 4b, 0 h). At 480-1520 h following initiation of the FR evolutionary experiment, parasites were amplified to levels equivalent to host replication. During 1520-2064 h, replication of both host and parasite declined. At 2848 and 3376 h, host replication increased modestly while parasite replication increased substantially. Parasite replication subsequently decreased at 3984 h, with both host self-replication activity and parasite replication declining at 4616 h.

We identified two notable patterns in host-parasite replication dynamics during the FR evolutionary experiment: 1) increased parasite replication (indicating loss of parasite resistance, e.g., at 480 and 2848 h) and 2) reduced replication for both host and parasite (suggesting parasite resistance coupled with diminished host replication ability, e.g., at 2064 and 4616 h).

The subsequent question was how these characteristics of evolved hosts and parasites resulted in reduced host RNA concentrations at the bottom of oscillation. In the evolutionary experiments, extinctions were frequently observed around 2000, 3000, and 4600 h. Host and parasite RNAs during these periods (2064, 2848, and 4616 h in Fig. 4b) exhibited two distinct characteristics: reduced host replication with parasite resistance (2064 and 4616 h), and elevated host replication with parasite susceptibility (2848 h). To test whether these two contrasting characteristics could result in lower host RNA concentrations at the bottom of oscillation, we conducted short-term replication experiments using host-parasite pairs from each time point (0, 2064, 2848, 3984 h) under the condition approximating FR condition (0.5 h reaction time and 0.5/round dilution rate), and quantified each host and parasite concentrations. These experiments were performed independently in triplicate (Fig. 4c). The average host concentration at the bottom are presented in Fig. 4d. The bottom concentration at 0 h exceeded 10^{-2} nM but decreased to below 10^{-2} nM for 2064, 2848, and 3984 h (Fig. 4d), indicating that all three evolved RNA pairs reduced the host concentrations at the bottom, consistent with frequent extinctions observed around these time periods.

Discussion

Coevolution between hosts and parasites represents an important evolutionary phenomenon relevant to the origin of life and the modern biology; however, experimental evidence regarding potential coevolutionary outcomes remains limited. Here, we conducted and analyzed a long-term evolutionary experiment under altered dilution frequency and demonstrated that the evolutionary outcome differed significantly from our previous evolutionary experiment. Host RNA exhibited a tendency toward extinction in later evolutionary stages (Fig. 1), and lost their lineage diversity (Fig. 2). Assays using RNA clones revealed that extended reaction times and moderate dilution rates were necessary for maintaining diversity (Fig. 3). Competition assay using isolated RNA clones demonstrated that RNAs selected during later stages exhibited two contrasting properties: high replication ability with low parasite resistance and low replication ability with high parasite resistance (Fig. 4b). Both properties were found to decrease the bottom host concentrations during oscillations (Figs. 4c and 4d), thereby increasing extinction probability. These results indicate that host-parasite coevolution does not invariably result in robust co-replication and spontaneous diversification, as observed in our previous evolutionary experiment, but can lead to diversity loss and increased extinction susceptibility depending on dilution conditions. These findings underscore the critical importance of environmental parameters that influence dilution dynamics for primitive replicators to evolve sustainably toward the emergence of life.

Although evolution is generally regarded as a process that either increases or maintains the fitness of populations of organisms or molecules, it can drive population extinction in theory, a phenomenon known as evolutionary suicide, runaway evolution, or Darwinian extinction[48,49]. Such evolution toward extinction has been investigated in several theoretical models[50–54], including predator-prey systems[55–57], bacterial populations[58], and epidemiological models[59,60]. However, experimental demonstration of evolution toward extinction remains limitting[61]. In this study, we provide an example of such evolution toward extinction using a molecular replication system. During the long-term evolutionary experiment under FR condition, we observed frequent extinctions only after 2000 h (Fig. 1c), suggesting that the host RNA evolved to acquire the characteristics that predispose it to extinction.

Our explanation for this counterintuitive evolutionary trajectory is as follows. First, the relatively short

reaction time under FR condition reduced diversity of RNA species, resulting in co-evolution of only one host and one parasite species (Fig. 3). In ecological studies, reduced diversity is known to enhance population fluctuations due to the absence of buffering effects from other species[43]. Additionally, host RNA evolved either to lose parasite resistance (2848 h and 3376 h in Fig. 4b) or to exhibit decreased self- replication ability (2064 h and 4616 h in Fig. 4b), both of which reduced host RNA concentrations at the bottom of oscillation (Fig. 4c). This population reduction could cause stochastic elimination of all RNAs, resulting in extinction. Similar extinction due to reduced population size during oscillations was observed in a previous theoretical study[44].

A remaining question is why host RNA evolved to lose parasite resistance or decrease its self-replication ability. Our proposed explanation is as follows. Under FR condition, dilution occurred more frequently than under SD condition. This frequent dilution is unfavorable for parasite because parasite replication requires coexistence with host RNA, potentially reducing the selective pressure for parasite resistance in host RNA. Consequently, parasite-susceptible hosts would dominate, as observed at 2848 h and 3376 h. However, when parasite-susceptible hosts dominated, parasitic RNA would be re-amplified despite unfavorable dilution conditions, placing the host under renewed selection pressure to increase parasite resistance. If host diversity were maintained and parasite-resistant hosts were present in the population, such parasite-resistant hosts would increase in frequency; however, in the FR experiment, host diversity was lost, requiring the remaining parasite-susceptible host to newly acquire parasite resistance. To acquire parasite resistance, host RNA must encode a replicase with specificity for the host sequence. Generally, there exists a trade-off between specificity and enzymatic activity in many proteins[62,63]. This trade-off may decrease self-replication ability together with parasite resistance, as observed at 2064 h and 4616 h. In summary, we propose that host-parasite coevolution under frequent dilution results in loss of host diversity, thereby selecting for RNA species that increased susceptibility to extinction.

Method

The translation-coupled RNA replication system

The translation-coupled RNA replication system used in this study originally consist of two components: a host RNA that encodes a core subunit of the Qβ RNA replicase gene with the recognition sequence, and the reconstituted translation system of *E. coli*, which contains all factors

323 required for translation, such as ribosome, translation proteins, tRNA, NTPs, and amino acids. The
324 components were prepared as previously described[64]. Parasitic RNAs appeared during the replication
325 from the host RNA.

326

327 **Evolutionary experiment using a flow reactor**

328 The droplet flow reactor system (Fig. S1) was constructed as described in a previous study[47]. This
329 system consisted of two 505 μL tanks set on magnetic stirrers. Oil phases and aqueous phases (the
330 reconstituted translation system) were supplied by syringe pumps into the 1st tank, where water-in-oil
331 droplets were prepared by stirring with a magnetic stirrer at 2 °C. The oil phase consisted of mineral
332 oil (Sigma) and surfactant, 2% Span 80 (Wako), and 3% Tween 80 (Wako), saturated with non-protein
333 components of the translation system, as described previously[18]. The prepared droplets were
334 transferred to the 2nd tank, in which the droplets contained host and parasitic RNAs, and RNA
335 replication occurred in the droplets at 37 °C. The droplets were mixed for 3 s every 60 s by stirring at
336 4800 rpm to induce fusion and division between the droplets. This corresponds to the low mixing
337 condition in a previous study[47]. The flow rate was 0.2/h (oil phase, 100 μL/h; aqueous phase, 1 μL/h).

338 At the start of the experiment, 500 μL of the oil phase and 5 μL of the translation system were added
339 to the 1st tank, and the emulsion was prepared by stirring at 2 °C and 7200 rpm for 10 min. The second
340 tank was filled with 505 μL of water-in-oil droplet, which was prepared by mixing droplets from round
341 155 of the previous SD evolutionary experiment with 4 μL of translation system and 400 μL of oil
342 phase at 7200 rpm for 3 min using a magnetic stirrer at 2 °C. When restarting the reaction in the middle
343 of this experiment, the water-in-oil droplets (505 μL) were added to the second tank at the restarting
344 time point. The translation system and oil phase were replenished every 2–3 days.

345

346 **RNA measurement**

347 To measure the host RNA concentration, the water-in-oil droplets were diluted 100-fold with 1 mM
348 EDTA (pH8.0) and heated at 95 °C for 5 min, followed by rapid cooling on ice. The heated sample
349 was then used for quantitative PCR after reverse transcription (RT-qPCR) using primers 1-4 and the
350 One-Step SYBR Prime Script PLUS RT-PCR Kit (Takara). To measure the parasitic RNA
351 concentration, the water phase was collected from 300 μL of the water-in-oil emulsion by
352 centrifugation at 15 krpm for 5 min. The precipitate was then washed with 120 μL of diethylether.

353 After centrifugation at 10 krpm for 1 min and removal of the ether phase, the remaining aqueous phase
354 was mixed with 50 μL of water, and RNA was purified using the RNeasy Mini Kit (QIAGEN). Purified
355 RNA (250 ng) was applied to an 8% polyacrylamide gel, as described previously[18]. As a size marker
356 for parasitic RNA, we used a short parasite (parasite α in a previous study[17] synthesized through *in*
357 *vitro* transcription. After electrophoresis at 150 V for 85 min, the gel was stained with SYBR Green II
358 (Takara). The intensity of each band was quantified using ImageJ software.

359

360 **Sequence analysis**

361 RNA was purified from the water-in-oil droplets as described above. Then, RNAs were reverse
362 transcribed with PrimeScript RTase (Takara) and primers 5 and 6, followed by RNase H (Takara)
363 treatment at 37 °C for 20 min. The cDNA was PCR-amplified using KOD FX (TOYOBO) and primers
364 5-6 and purified using the PureLink PCR Micro Kit (Life Technologies). The DNA corresponding to
365 the host and parasite were then separated by gel extraction using an E-gel agarose electrophoresis
366 system (Life Technologies), and barcode sequences were attached by PCR with KOD FX (TOYOBO)
367 and primers 5 and 6 attached to each barcode sequence. Then, the DNA mixture was sequenced using
368 PacBio Sequel. In PacBio Sequel, a single DNA molecule can be read multiple times owing to its
369 circular format. We used a consensus sequence of Q > 20 to reduce sequencing error. The number of
370 consensus sequence used was 10000 at any analyzed time point, except for parasites at 2848 h, 3376
371 h, and 3984 h. These three points were thought to have insufficient RNA concentrations; however,
372 more than 2,000 sequences were obtained. Following the method described in a previous study[18], 130
373 dominant mutations that existed at a frequency of 10% or higher in all the analyzed samples were
374 identified (Figs. S3 and S4). We classified the genotypes of each consensus sequence based only on
375 the dominant mutations because each consensus sequence contains many unique mutations, probably
376 because of the error-prone nature of RNA replication and the remaining sequencing errors. The
377 genotypes that were observed in more than nine reads were used for the following analysis. The
378 extracted genotypes and their frequencies are shown in Source Data file. Phylogenetic trees were
379 constructed using the top three most frequent genotypes from each analysis time point using the
380 neighbor-joining method in MEGA-X ver. 10.2.5[65].

381

382

383 **Coexistence experiment in Fig. 3**

384 The five RNA clones (three types of host RNA and two types of parasite RNA) found in the final
385 round (round 228) of the previous evolutionary experiment (HL1-228, HL2-228, HL3-228, PL2-228,
386 and PL3-228) were prepared by in vitro transcription as described previously[18]. The five RNA clones
387 were mixed at 10 nM each in the translation system, and the mixture (10 μL) and the buffer-saturated
388 oil phase (990 μL) were vigorously mixed with a homogenizer (Polytron PT-1300D, KINEMATICA)
389 to prepare water-in-oil droplets. The droplets were incubated at 37 °C for the indicated periods and
390 diluted with water-in-oil droplets, which were prepared by mixing the saturated oil and translation
391 system, at the indicated dilution ratio using the same method without RNA addition. The diluted
392 droplets were further incubated for the next round of replication, for the indicated periods. After
393 repeating this serial dilution process, each RNA sample was measured using RT-qPCR with specific
394 primers 7-16 and the One Step SYBR PrimeScript PLUS RT-PCR Kit (Takara). Although we used
395 primers that selectively recognized only one of the five RNA clones, a low level of misrecognition
396 occurred (usually 1/100 – 1/1000 of the legitimate recognition) (Fig. S7). This misrecognition effect
397 was subtracted when calculating RNA concentration. For the round 155 RNA set, because sufficient
398 accuracy could not be achieved with one-step RT-qPCR, only the plus strand was measured using
399 primers 17-24. Primer sequences are shown in Source Data file.

400

401

402 **Coexistence simulation in Fig. 3**

403 The simulation was based on the replication-mixing-dilution model described in a previous study[18].
404 This model consists of three steps, 1) replication, 2) dilution, and 3) fusion-division, and 300,000
405 droplets (compartments). 1) In the replication step, i^{th} RNA species replicate logistically in each
406 droplet, according to the differential equations described below.

407 $$\frac{dRNA_i}{dt} = RNA_i \sum_{j=1}^{5} k_{ij} RNA_j \left(1 - \frac{\sum_{h=1}^{5} RNA_h}{C}\right),$$

408 where C is a carrying capacity in a droplet (300). The replication rate constants k_{ij}, experimentally
409 determined previously[18], were multiplied by 0.1 in this study because the original values were too
410 large to observe the effect of the reaction time. 2) In the next dilution step, the droplets were randomly

411 removed according to the dilution rate, and an equal number of empty droplets were added. 3) In the
412 subsequent fusion-division step, RNAs from two randomly selected droplets were combined and
413 redistributed into two new droplets according to a binomial distribution to mimic the fusion-division
414 process of droplets. This process was repeated 1.3 times the droplet number according to the previous
415 study. Starting from an initial state in which RNAs were distributed according to a Poisson distribution
416 with a mean of 10 molecules per droplet, the replication, dilution, and redistribution processes were
417 repeated for 50 rounds. All parameter values used in this simulation are shown in Source Data file.

418

419 **Rationale of the incubation time and dilution rate under the SD and FR conditions**

420 The condition corresponding to the previous evolutionary experiment (SD condition) was a reaction
421 time of 5 h and a dilution rate of 0.8 /round because one round of serial dilution cycle consisted of
422 incubation for 5 h, followed by 5-fold dilution.

423 The condition close to the new evolutionary experiment using the flow reactor (FR condition) is a
424 reaction time of 0.5 h and a dilution rate of 0.5 /round for the following reasons. Under FR condition,
425 we stirred the droplets at a 5% duty ratio, which corresponds to a diffusion coefficient of 0.35 /min^{-1},
426 which means that droplets experience a fusion-division event approximately once every 0.5 h
427 according to the data in a previous study[66] (based on Fig. 4 of the previous study). Therefore, we
428 adopted a continuous reaction time before dilution of 0.5 /h. In addition, RNA in a droplet should be
429 diluted 1/2 in a single fusion-division event, assuming that all droplets are same size and a fusion-
430 division event of two droplets mixes the contents completely and produces two droplets of the same
431 size. Therefore, we chose a reaction time of 0.5 h and a dilution rate of 0.5 /round for that close to FR
432 condition. It should be noted that the above calculation is valid only when the concentration of RNA-
433 containing droplets is low and fusion between such droplets is negligible. When the concentration of
434 RNA-containing droplets becomes high, the effective dilution rate approaches that of the reaction tank
435 itself (20% /h, Fig. 1b), corresponding to 0.1 per round at 0.5 h reaction time. Therefore, the dilution
436 rate of 0.5 per round used in this study may represent an overestimation.

437

438 **Competition assay conducted in Fig. 4b**

439 Representative RNAs (the most frequent genotype) at each time point were used in the co-replication
440 assay. The RNA clones were prepared as follows: The PCR amplified cDNA was ligated to a vector,

441 pUC19 or pBAD33, using In-Fusion HD Enzyme Premix (Takara), and amplified in *E. coli* DH5α.
442 We checked the sequence using Sanger sequencing, and if there were any unintended mutations, we
443 corrected them using whole plasmid PCR with primers containing corrected mutations, followed by
444 ligation and transformation as described above. The plasmids containing correct RNA sequence were
445 digested with Sma I (Takara) to determine the 3'-end of RNA, transcribed using T7 RNA polymerase
446 (Takara), and purified using the RNeasy Mini Kit (QIAGEN). DNAs was degraded using DNase I
447 (RNase-free) (Takara) treatment, and the RNAs were purified using the RNeasy Mini Kit (QIAGEN).
448 Each host and parasite RNA clones (1 nM) are mixed in the reconstituted translation system and
449 incubated at 37 °C for 1 h. The concentrations of the host and parasite RNA were measured by RT-
450 qPCR with specific primers. Primer sequences are shown in Source Data file.

451

452 **Assay of the bottom concentration conducted in Fig. 4c**

453 Each indicated host and parasite RNA clones were mixed at 10 nM each in the translation system, and
454 the mixture (10 μL) was homogenized in the buffer-saturated oil phase to prepare water-in-oil droplets
455 as described above in the coexistence experiment section. The serial dilution cycle was repeated 38–
456 40 times under the condition close to FR condition (0.5 h reaction time and 0.5 /round dilution rate)
457 as described in the same section.

458

459 **Calculation of generations**

460 In the FR evolutionary experiment, the host RNA concentration was maintained for 5000 h while
461 exchanging 20% of the reaction mixture per hour. Consequently, host RNAs underwent 1.25-fold
462 replication per hour, resulting in 1.25^{5000}-fold amplification at 5000 h. We defined one generation for
463 an RNA replicator as the time required to double. Therefore, the total number of generations was
464 calculated as $\log_2(1.25^{5000}) \sim 15{,}000$.

465

466 **Supplementary Materials**

467 Extended Data Figures, Supplementary Discussion, and Source Data for this article is available.

468

Acknowledgements:

We thank Mrs. Kayo Aoyama and Ayu Saito for technical support.

Funding:

This work was supported by JST, CREST Grant Number JPMJCR20S1, Japan, and Kakenhi Grant Numbers 24H00573 and 24H01111.

Author contributions:

TY performed the evolutionary experiments and KY design and performed the other experiments. RM and NI design experiments. NI and KY wrote the manuscript.

Competing interests:

The authors declare that they have no conflicts of interest.

Data and materials availability:

The data are available upon request from the authors.

Reference

1. Szathmáry, E. & John Maynard, S. The major evolutionary transitions. *Nature* **374**, 227–232 (1995).
2. Joyce, G. F. The antiquity of RNA-based evolution. *Nature* **418**, 214–221 (2002).
3. Koonin, E. V. & Martin, W. On the origin of genomes and cells within inorganic compartments. *Trends in Genetics* **21**, 647–654 (2005).
4. Yarus, M. Getting past the RNA world: The initial Darwinian ancestor. *Cold Spring*

Harb Perspect Biol **3**, 1–8 (2011).

5. Pross, A. & Pascal, R. The origin of life: What we know, what we can know and what we will never know. *Open Biol* **3**, 1–5 (2013).

6. Higgs, P. G. & Lehman, N. The RNA World: molecular cooperation at the origins of life. *Nat Rev Genet* **16**, 7–17 (2015).

7. Goldenfeld, N., Biancalani, T. & Jafarpour, F. Universal biology and the statistical mechanics of early life. *Philosophical Transactions of the Royal Society A: Mathematical, Physical and Engineering Sciences* **375**, 1–14 (2017).

8. Adamski, P. *et al.* From self-replication to replicator systems en route to de novo life. *Nat Rev Chem* **4**, 386–403 (2020).

9. Brunk, C. F. & Marshall, C. R. 'Whole Organism', Systems Biology, and Top-Down Criteria for Evaluating Scenarios for the Origin of Life. *Life* **11**, 690 (2021).

10. Mills, D. R., Peterson, R. L. & Spiegelman, S. An extracellular Darwinian experiment with a self-duplicating nucleic acid molecule. *Proc Natl Acad Sci U S A* **58**, 217–224 (1967).

11. Breaker, R. R. & Joyce, G. F. Emergence of a replicating species from an in vitro RNA evolution reaction. *Proceedings of the National Academy of Sciences* **91**, 6093–6097 (1994).

12. Wright, M. C. & Joyce, G. F. Continuous in vitro evolution of catalytic function. *Science (1979)* **276**, 614–617 (1997).

13. Voytek, S. B. & Joyce, G. F. Niche partitioning in the coevolution of 2 distinct RNA enzymes. *Proc Natl Acad Sci U S A* **106**, 7780–7785 (2009).

14. Kramer, F. R., Mills, D. R., Cole, P. E., Nishihara, T. & Spiegelman, S. Evolution in vitro: Sequence and phenotype of a mutant RNA resistant to ethidium bromide. *J Mol Biol* **89**, 719–736 (1974).

15. Paegel, B. M. & Joyce, G. F. Microfluidic compartmentalized directed evolution. *Chem Biol* **17**, 717–724 (2010).

16. Ichihashi, N. *et al.* Darwinian evolution in a translation-coupled RNA replication system

within a cell-like compartment. *Nat Commun* **4**, 2494 (2013).

17. Furubayashi, T. *et al.* Emergence and diversification of a host-parasite RNA ecosystem through Darwinian evolution. *Elife* **9**, (2020).

18. Mizuuchi, Ryo., Furubayashi, Taro. & Ichihashi, Norikazu. Evolutionary transition from a single RNA replicator to a multiple replicator network. *Nat Commun* **13**, 1460 (2022).

19. Iranzo, J., Puigbo, P., Lobkovsky, A. E., Wolf, Y. I. & Koonin, E. V. Inevitability of genetic parasites. *Genome Biol Evol* **8**, 2856–2869 (2016).

20. Eigen, M. & Schuster, P. The Hypercycle: Part C. *Naturwissenschaften* **65**, 341–369 (1978).

21. Maynard Smith, J. Hypercycles and the origin of life. *Nature* **280**, 445–446 (1979).

22. Bresch, C., Niesert, U. & Harnasch, D. Hypercycles, parasites and packages. *J Theor Biol* **85**, 399–405 (1980).

23. Szathmáry, E. & Demeter, L. Group selection of early replicators and the origin of life. *J Theor Biol* **128**, 463–86 (1987).

24. Furubayashi, T. & Ichihashi, N. Sustainability of a compartmentalized host-parasite replicator system under periodic washout-mixing cycles. *Life* **8**, 3 (2018).

25. Laurent, G., Peliti, L. & Lacoste, D. Survival of self-replicatingmolecules under transient compartmentalization with natural selection. *Life* **9**, 78 (2019).

26. Blokhuis, A., Nghe, P., Peliti, L. & Lacoste, D. The generality of transient compartmentalization and its associated error thresholds. *J Theor Biol* **487**, 110110 (2020).

27. Matsumura, S. *et al.* Transient compartmentalization of RNA replicators prevents extinction due to parasites. *Science (1979)* **354**, 1293–1296 (2016).

28. Bianconi, G., Zhao, K., Chen, I. A. & Nowak, M. A. Selection for Replicases in Protocells. *PLoS Comput Biol* **9**, e1003051 (2013).

29. Boerlijst, M. C. & Hogeweg, P. Spiral wave structure in pre-biotic evolution: hypercycles stable against parasites. *Physica D* **48**, 17–28 (1991).

30. Boerlijst, M. C. & Hogeweg, P. Spatial gradients enhance persistence of hypercycles. *Physica D* **88**, 29–39 (1995).

31. Cronhjort, M. B. & Blomberg, C. Cluster compartmentalization may provide resistance to parasites for catalytic networks. *Physica D* **101**, 289–298 (1997).

32. McCaskill, J. S., Füchslin, R. M. & Altmeyer, S. The stochastic evolution of catalysts in spatially resolved molecular systems. *Biol Chem* **382**, 1343–1363 (2001).

33. Szabó, P., Scheuring, I., Czárán, T. & Szathmáry, E. In silico simulations reveal that replicators with limited dispersal evolve towards higher efficiency and fidelity. *Nature* **420**, 340–343 (2002).

34. Sardanyés, J. & Solé, R. V. Spatio-temporal dynamics in simple asymmetric hypercycles under weak parasitic coupling. *Physica D* **231**, 116–129 (2007).

35. Shay, J. A., Huynh, C. & Higgs, P. G. The origin and spread of a cooperative replicase in a prebiotic chemical system. *J Theor Biol* **364**, 249–259 (2015).

36. Levin, S. R. & West, S. A. The evolution of cooperation in simple molecular replicators. *Proceedings of the Royal Society B: Biological Sciences* **284**, 1–8 (2017).

37. Levin, S. R., Gandon, S. & West, S. A. The social coevolution hypothesis for the origin of enzymatic cooperation. *Nat Ecol Evol* **4**, 132–137 (2020).

38. Buckingham, L. J. & Ashby, B. Coevolutionary theory of hosts and parasites. *J Evol Biol* **35**, 205–224 (2022).

39. Takeuchi, N. & Hogeweg, P. Evolution of complexity in RNA-like replicator systems. *Biol Direct* **3**, 1–20 (2008).

40. Seoane, L. F. & Solé, R. How Turing parasites expand the computational landscape of digital life. *Phys Rev E* **108**, 044407 (2023).

41. Zaman, L. *et al.* Coevolution Drives the Emergence of Complex Traits and Promotes Evolvability. *PLoS Biol* **12**, e1002023 (2014).

42. Hickinbotham, S. J., Stepney, S. & Hogeweg, P. Nothing in evolution makes sense except in the light of parasitism: evolution of complex replication strategies. *R Soc Open Sci* **8**, 210441 (2021).

43. Decaestecker, E., De Gersem, H., Michalakis, Y. & Raeymaekers, J. A. M. Damped long-term host-parasite Red Queen coevolutionary dynamics: A reflection of dilution effects? *Ecol Lett* **16**, 1455–1462 (2013).

44. Gokhale, C. S., Papkou, A., Traulsen, A. & Schulenburg, H. Lotka-Volterra dynamics kills the Red Queen: population size fluctuations and associated stochasticity dramatically change host-parasite coevolution. *BMC Evol Biol* **13**, 254 (2013).

45. Brockhurst, M. A. & Koskella, B. Experimental coevolution of species interactions. *Trends Ecol Evol* **28**, 367–375 (2013).

46. Kamiura, R., Mizuuchi, R. & Ichihashi, N. Plausible pathway for a host-parasite molecular replication network to increase its complexity through Darwinian evolution. *PLoS Comput Biol* **18**, e1010709 (2022).

47. Yoshiyama, T., Ichii, T., Yomo, T. & Ichihashi, N. Automated in vitro evolution of a translation-coupled RNA replication system in a droplet flow reactor. *Sci Rep* **8**, 11867 (2018).

48. Webb, C. A Complete Classification of Darwinian Extinction in Ecological Interactions. *Am Nat* **161**, 181–205 (2003).

49. Kalle Parvinen. Evolutionary Suicide. *Acta Biotheor* **53**, 241–264 (2005).

50. Ferrière, R. Adaptive responses to environmental threats: evolutionary suicide, insurance, and rescue. in *Options Spring* 12–16 (IIASA, Laxenburg, Austria, 2000).

51. Gyllenberg, M. & Parvinen, K. Necessary and sufficient conditions for evolutionary suicide. *Bull Math Biol* **63**, 981–993 (2001).

52. Parvinen, K. Evolutionary suicide in a discrete-time metapopulation model. *Evol Ecol Res* **9**, 619–633 (2007).

53. Parvinen, K. Adaptive dynamics of cooperation may prevent the coexistence of defectors and cooperators and even cause extinction. *Proceedings of the Royal Society B: Biological Sciences* **277**, 2493–2501 (2010).

54. Parvinen, K. & Dieckmann, U. Self-extinction through optimizing selection. *J Theor Biol* **333**, 1–9 (2013).

55. Matsuda, H. & Abrams, P. A. Runaway evolution to self-extinction under asymmetrical competition. *Evolution (N Y)* **48**, 1764–1772 (1994).

56. Hiroyuki Matsuda & Peter A. Abrams. Timid Consumers: Self-Extinction Due to Adaptive Change in Foraging and Anti-predator Effort. *Theor Popul Biol* **45**, 76–91 (1994).

57. Dieckmann, U., Marrow, P. & Law, R. Evolutionary Cycling in Predator-Prey Interactions: Population Dynamics and the Red Queen. *Jouranal of Theoretical Biology* **176**, 91–102 (1995).

58. Himeoka, Y. & Mitarai, N. Dynamics of bacterial populations under the feast-famine cycles. *Phys Rev Res* **2**, 013372 (2020).

59. Boots, M. & Sasaki, A. Parasite evolution and extinctions. *Ecol Lett* **6**, 176–182 (2003).

60. Boldin, B. & Kisdi, É. Evolutionary suicide through a non-catastrophic bifurcation: adaptive dynamics of pathogens with frequency-dependent transmission. *J Math Biol* **72**, 1101–1124 (2016).

61. Rankin, D. J. & López-Sepulcre, A. Can adaptation lead to extinction? *Oikos* **111**, 616–619 (2005).

62. Tawfik, D. S. Accuracy-rate tradeoffs: How do enzymes meet demands of selectivity and catalytic efficiency? *Curr Opin Chem Biol* **21**, 73–80 (2014).

63. Jana, T., Brodsky, S. & Barkai, N. Speed–Specificity Trade-Offs in the Transcription Factors Search for Their Genomic Binding Sites. *Trends in Genetics* **37**, 421–432 (2021).

64. Hagino, K., Masuda, K., Shimizu, Y. & Ichihashi, N. Sustainable regeneration of 20 aminoacyl-tRNA synthetases in a reconstituted system toward self-synthesizing artificial systems. *Sci Adv* **11**, 6269 (2025).

65. Kumar, S., Stecher, G., Li, M., Knyaz, C. & Tamura, K. MEGA X: Molecular evolutionary genetics analysis across computing platforms. *Mol Biol Evol* **35**, 1547–1549 (2018).

66. Yoshiyama, T., Motohashi, C., Ichihashi, N., Ichii, T. & Yomo, T. Maintenance of a translation-coupled RNA replication in dynamic micro-sized compartments under

continuous stirring and flow. *Chemical Engineering Journal* **283**, 896–902 (2016).

Figures

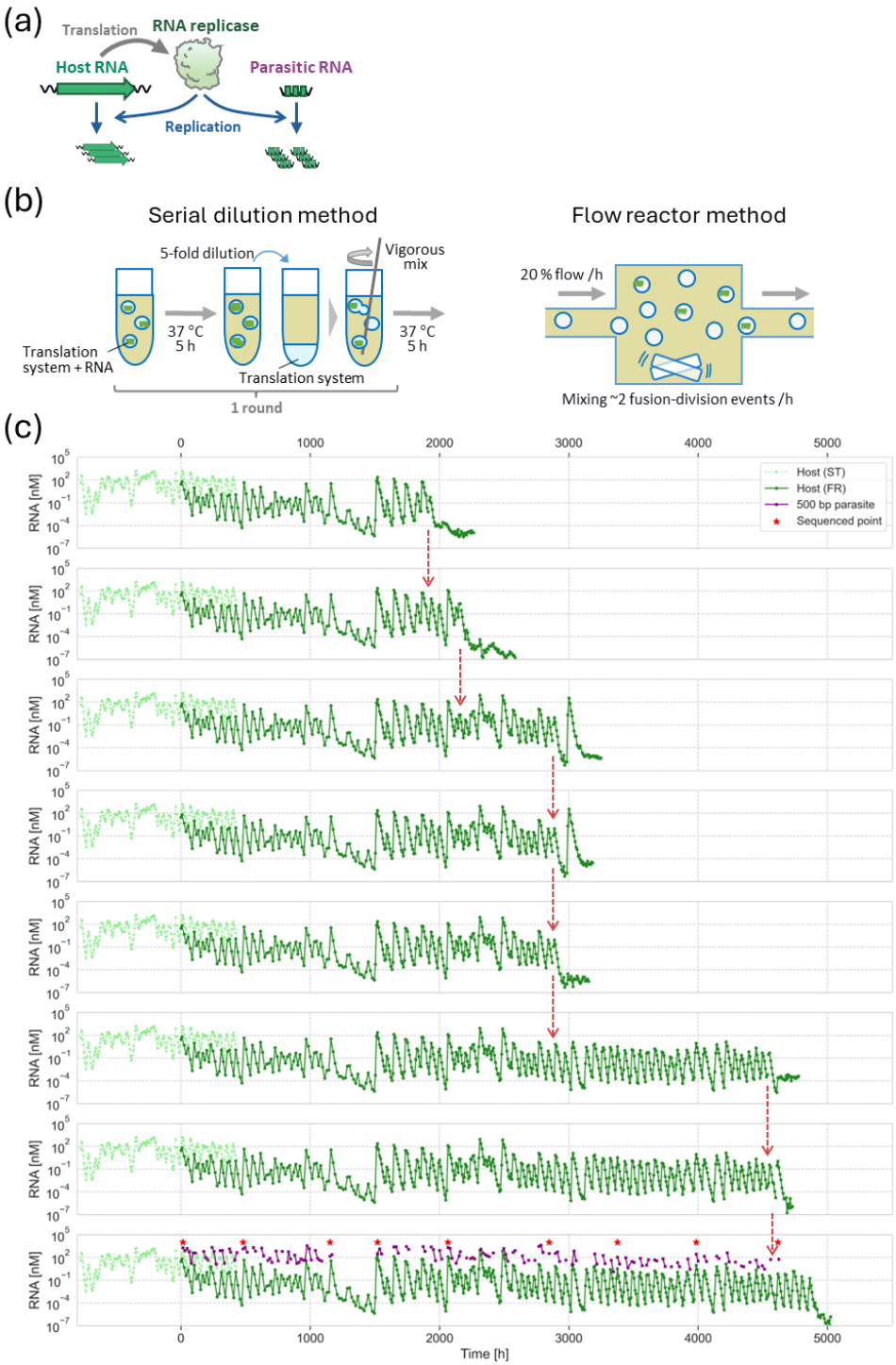

Figure 1: A long-term experiment using a flow reactor.

(a) Scheme of translation-coupled RNA replication. RNA replicase is translated into a host RNA and

replicates both host and parasitic RNA. (b) Differences between previous serial dilution (SD) and new flow reactor (FR) methods. In the SD method, water-in-oil droplets containing the host and parasite RNA and the translation system were incubated for 5 h at 37°C for RNA replication. Then, an aliquot of the droplets was diluted to 5-fold with new oil phage and the translation system, vigorously mixed to prepare new droplets with completely mixed contents, and incubated for 5 h at 37°C again for the next round of replication. In FR method, water-in-oil droplets were incubated at 37°C and stirred for 3 s every 60 s, which allows approximately 2 fusion-division events /h. New droplets containing the translation system were supplied constantly at a rate of exchange of 20% of the total volume per hour. (c) Trajectories of host RNA concentration during the FR evolutionary experiment until each extinction. The host RNA concentrations were measured by RT-qPCR using host-specific but lineage-nonspecific primers. The results of previous evolutionary experiment under SD condition from rounds 0 to 240 are shown in light green, assuming that one round was equivalent to five hours. The new evolutionary experiment under FR condition was started from the RNA population of round 155 under SD condition, and the results are shown in deep green. When the host dropped below the detection limit multiple times and did not recover, the experiment was restarted from the stocked sample at an earlier time point (indicated by the red dotted arrows). Parasitic RNA concentrations, measured by quantification from SDS-PAGE images, are shown in the bottom panel (purple makers). The time points used for sequence analysis are indicated by red stars.

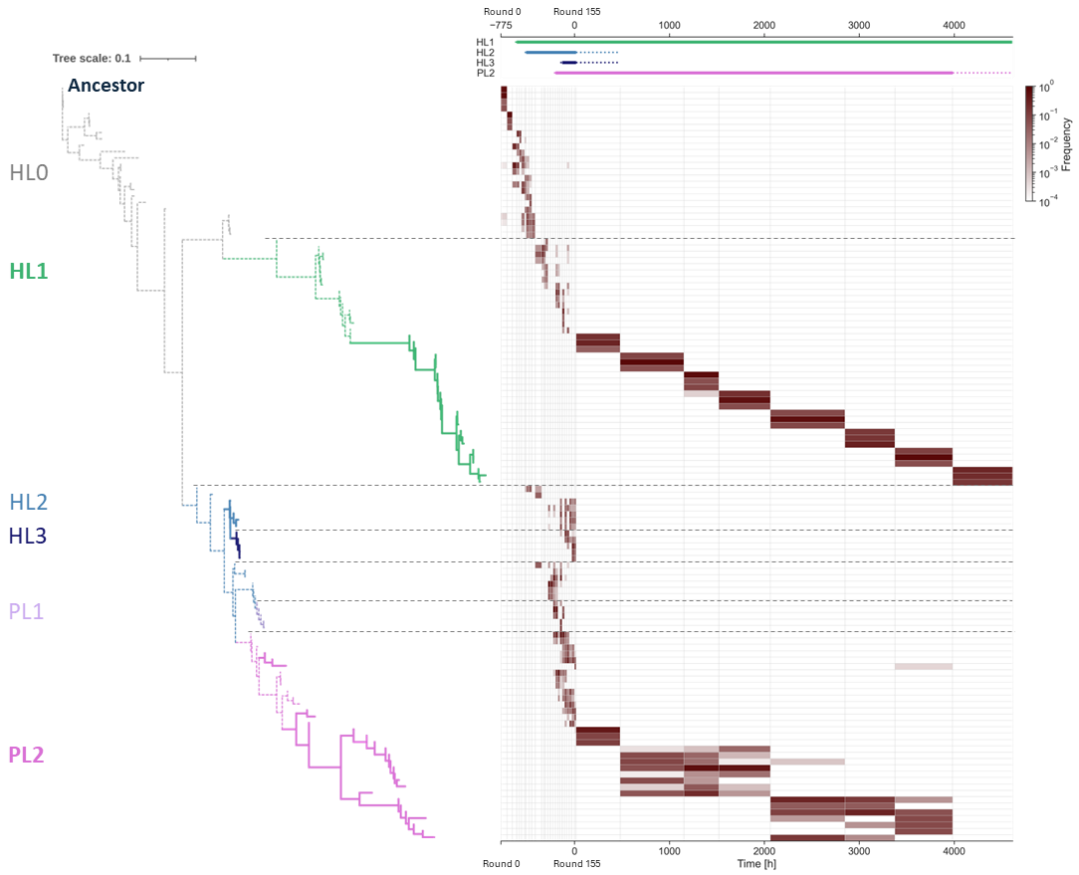

Figure 2: Phylogenetic tree and frequencies in the population

(a) A phylogenetic tree was constructed using the three most frequent genotypes at each sequencing time point. The branches for the previous SD experiment (until round 155) and new RF experiment are shown as dashed and solid lines, respectively. Different types of RNA are depicted in different colors based on the classification in a previous study[18]. The heatmap shows the frequencies of the genotypes in each branch. (b) Schematic representation of existing RNA lineages. Uncertain regions due to the lack of sequence data were shown in dotted lines.

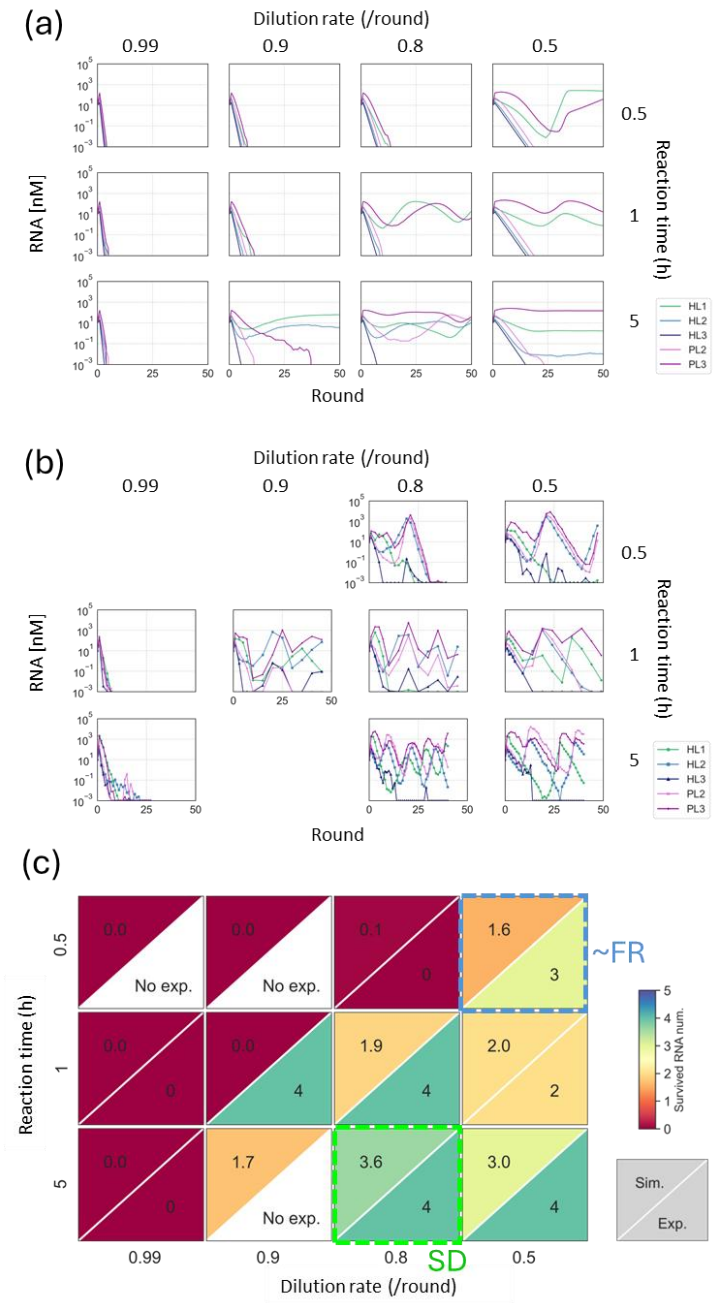

Figure 3: Effect of dilution rate and reaction time on coexistence of multiple host and parasitic RNA

Short-term serial dilution experiment with five types of RNA species (three hosts and two parasites) were performed for 40 – 50 rounds at different dilution rates and reaction times using both computer simulations (a) and experiments (b). (c) Summary of the number of RNA species in the final population in the simulation (top left, average of 20 runs) and the experiment (bottom right).

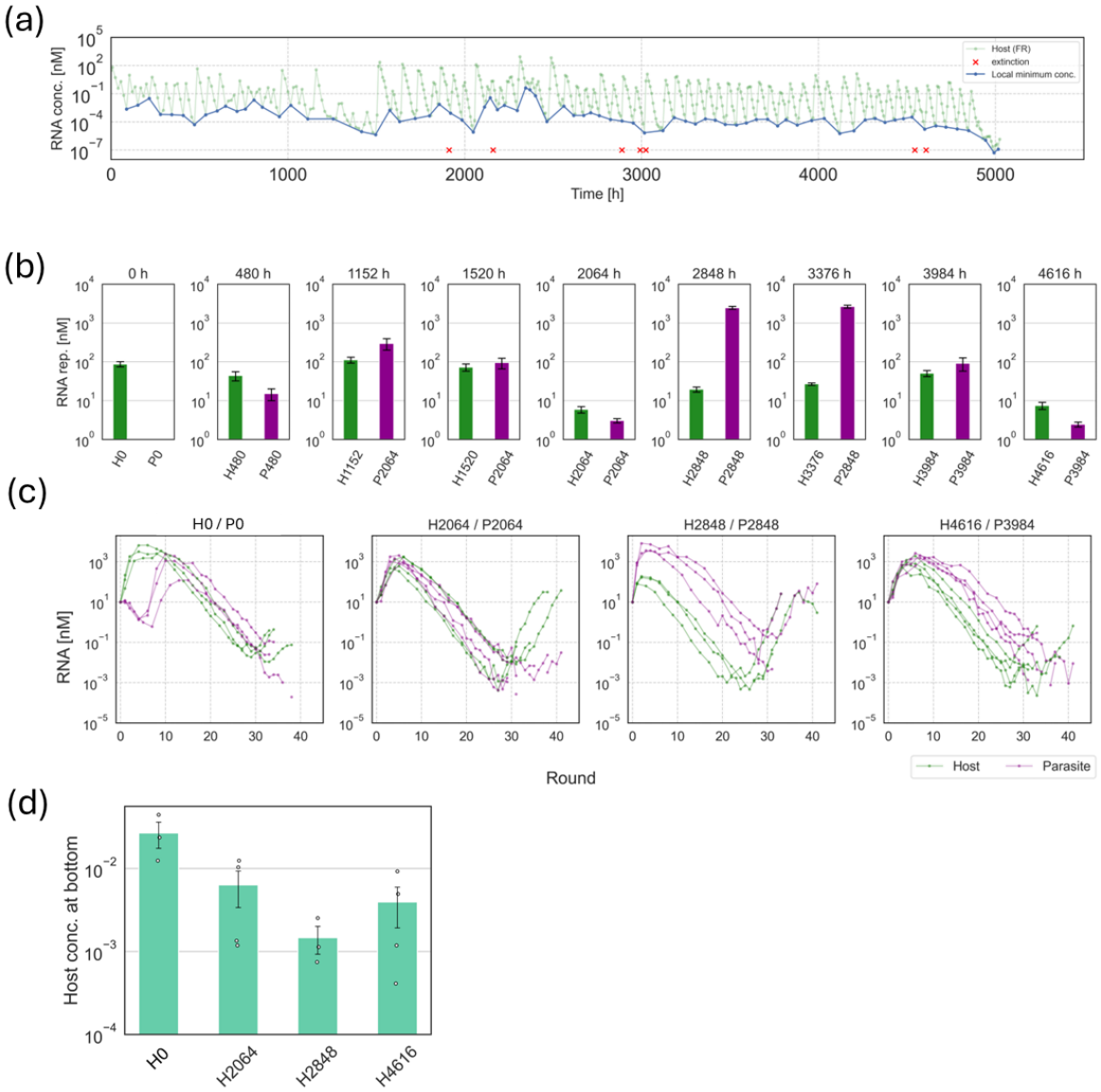

Figure 4: Characterization of RNA species that appeared in the FR evolutionary experiment.

(a) Trajectory of the host RNA concentrations at the bottom of oscillation. (b) Competition experiments with a host and parasitic RNA clones that dominated at the indicated time points. Each RNA pair (1 nM each) was incubated in the translation system at 37 °C for 1 h, and the host and parasite concentrations were measured using RTqPCR. (c) A short-term serial dilution experiment using the host and parasite RNA pairs (10 nM each) at 0, 2026, 2848, and 4616 h under the condition close to FR condition (0.5 h reaction time and 0.5 /round dilution rate) for 38–40 rounds. The average host RNA concentrations at the bottom are shown in (d) with standard errors (N = 3 or 4).